

Factors Influencing Ductility in the Superplastic Zn-22 Pct Al Eutectoid

FARGHALLI A. MOHAMED, MOHAMED M. I. AHMED, AND TERENCE G. LANGDON

The maximum attainable ductility in the superplastic Zn-22 pct Al eutectoid depends critically on the imposed strain rate, the testing temperature, and the initial grain size. High ductilities are observed at intermediate strain rates, and there is a decrease at both higher and lower rates of strain. It is shown that i) the maximum ductility occurs at higher strain rates as the temperature is increased and/or the initial grain size is decreased, and ii) the maximum attainable ductility increases with increasing temperature and/or decreasing initial grain size. For specimens tested at different temperatures, similar macroscopic fracture characteristics are observed in specimens exhibiting a similar maximum flow stress. The experimental trends are qualitatively explained by relating maximum ductility to the maximum strain rate sensitivity and examining the influence of cavitation on the time to rupture.

SUPERPLASTIC materials are usually tested under tensile conditions, and the flow stress, σ , is then related to the imposed strain rate, $\dot{\epsilon}$, by an empirical equation of the form

$$\sigma = B \dot{\epsilon}^m \quad [1]$$

where B is a constant for any given testing conditions and m is the strain rate sensitivity. The value of m is equivalent to the reciprocal of the stress exponent, n , in the standard relationship for steady-state creep.

A detailed investigation of the mechanical characteristics of the superplastic Zn-22 pct Al eutectoid has produced a comprehensive set of experimental results, of which the three primary findings may be briefly summarized as under:

i) There is a sigmoidal relationship between stress and strain rate, such that the value of m is ~ 0.25 at very low strain rates ($\lesssim 10^{-5} \text{ s}^{-1}$, Region I), increases to ~ 0.45 at intermediate strain rates ($\sim 10^{-5} - 10^{-2} \text{ s}^{-1}$, Region II), and then decreases again at high rates of strain ($\gtrsim 10^{-2} \text{ s}^{-1}$, Region III).¹

ii) The activation energy for plastic flow is close to that of lattice diffusion in Region I, but decreases to a value similar to that anticipated for grain boundary diffusion in Region II, and then increases again in Region III.²

iii) For specimens having an average grain size of $2.5 \mu\text{m}$ tested at a temperature of 473 K, the percentage elongation of each specimen at fracture increases from <500 pct in Region I, reaches a value >2000 pct in Region II, and then decreases to <500 pct in Region III.³

These results show clearly that the superplastic properties of the Zn-22 pct Al eutectoid are optimized within a narrow range of strain rate where the value of m is a maximum and the activation energy is relatively low, and the superplastic characteristics are lost at both higher and lower rates of strain. The present work was therefore undertaken to investigate in more detail the precise influence of temperature

and grain size on the total ductility in this superplastic alloy.

EXPERIMENTAL PROCEDURE

Sheets of the Zn-22 pct Al eutectoid alloy, 0.254 cm in thickness, were obtained in superplastic form from The New Jersey Zinc Company. This material, known commercially as Super-Z 200, had an as-received grain size of the order of $1 \mu\text{m}$. Tensile specimens, having a gage length of 0.635 cm, were cut from the sheets, and the specimens were then annealed for different times at 533 K to give average equiaxed spatial grain diameters, d (defined as $1.74 \times$ the mean linear intercept), of 2.5 and $4.2 \mu\text{m}$, respectively. The accuracy of these, and subsequent, grain size measurements was ± 10 pct. A typical photomicrograph of a longitudinal section of the $2.5 \mu\text{m}$ material is shown in Fig. 1.

The specimens were tested on an Instron testing machine having a constant rate of cross-head displacement: the strain rates quoted herein therefore refer to *initial* strain rates, calculated from the initial gage length of the specimen. The Instron machine was equipped with a high speed (0.25 s) recorder pen to facilitate measurements at very rapid strain rates.

A uniform temperature was maintained over the en-

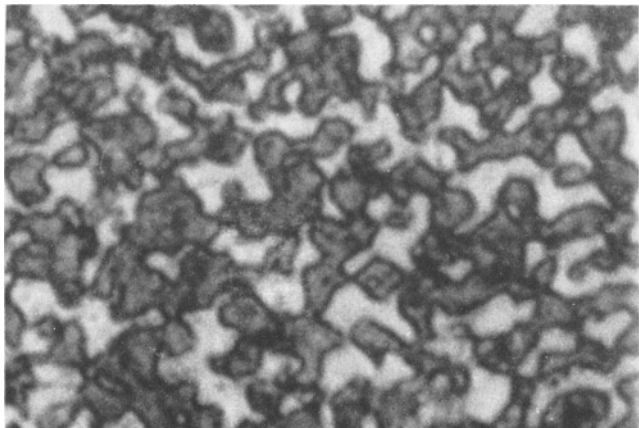


Fig. 1—Microstructure of the Zn-22 pct Al alloy prior to testing. Average grain size $d = 2.5 \mu\text{m}$. Magnification 1860 times.

FARGHALLI A. MOHAMED, MOHAMED M. I. AHMED, and TERENCE G. LANGDON are Assistant Professor, Graduate Research Assistant, and Professor, respectively, Department of Materials Science, University of Southern California, Los Angeles, CA 90007.

Manuscript submitted July 16, 1976.

tire specimen gage length, even at very high elongations, by immersing the specimens in a silicone oil bath which was electrically heated and stirred with bubbling argon. The bath temperature was continuously monitored with chromel-alumel thermocouples and maintained constant to ± 1 K.

All specimens were pulled to fracture at a single rate of cross-head displacement. After fracture, longitudinal sections of the gage length of several of the specimens were prepared metallographically for measurements of the final grain size.

EXPERIMENTAL RESULTS

Effect of Temperature

Fig. 2 shows the experimental results obtained at 423 and 503 K with an initial grain size of $2.5 \mu\text{m}$, together with the datum points reported earlier by Ishikawa *et al.*³ for a temperature of 473 K.

The lower portion of Fig. 2 shows the maximum observed flow stress plotted as a function of the initial strain rate. These curves exhibit the characteristic sigmoidal shape reported earlier for Zn-22 pct Al (Ref. 1) and Pb-62 pct Sn,⁴ so that the curves divide readily into three distinct regions of behavior. The strain rate sensitivity, m , is ~ 0.22 at very low values of the imposed strain rate (Region I), increases to ~ 0.5 at intermediate strain rates (Region II), and then decreases again at high strain rates (Region III).

The upper portion of Fig. 2 shows the percentage

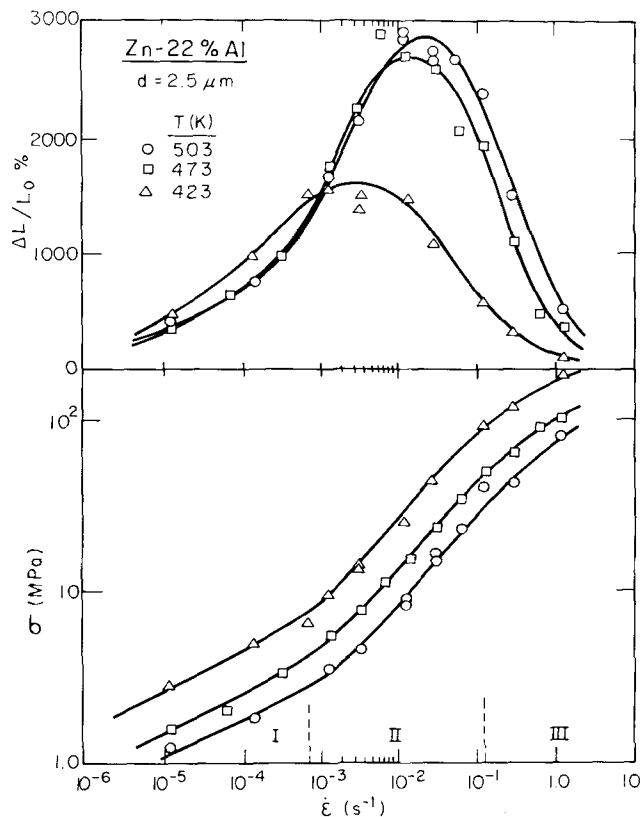


Fig. 2—Tensile fracture strain as a percentage *vs* initial strain rate for an initial grain size of $2.5 \mu\text{m}$ and testing temperatures of 423, 473, and 503 K (upper); the corresponding plots of maximum flow stress *vs* initial strain rate (lower).

elongation of each specimen at fracture, $\Delta L/L_0$ pct, as a function of strain rate, where ΔL is the total increase in length at the point of failure and L_0 is the initial gage length of the specimen.

Although there is some scatter in the individual datum points, these experimental curves reveal four significant features:

- i) Maximum ductility occurs over an intermediate range of strain rate, and there is a decrease in the strain to failure at both high and low values of $\dot{\epsilon}$.
- ii) As the testing temperature is increased, the peak in the curve of $\Delta L/L_0$ *vs* $\dot{\epsilon}$ occurs at higher strain rates.
- iii) The maximum attainable ductility in the superplastic region increases with increasing temperature.
- iv) Maximum ductility occurs at the highest testing temperature at high strain rates, but at low strain rates this trend is reversed.

At the macroscopic level, a marked difference in appearance was observed in the fractured specimens tested at different strain rates. This may be appreciated by a comparison of the various specimens after fracture, as shown in Figs. 3 and 4 for testing temperatures of 423 and 503 K, respectively. In Figs. 3 and 4, Specimen A is untested, and Specimens B to J were pulled to failure under decreasing rates of strain.

At the lowest temperature and highest strain rate, failure occurred in a quasi-brittle manner with little or no necking and an overall ductility of ~ 70 pct (Specimen B in Fig. 3). As the initial strain rate was decreased at this temperature, the specimens began to exhibit larger strains and ultimately, in the superplastic range, pulled out to a fine point (Specimens F, G, and H in Fig. 3). At even lower strain rates, the ductility was limited by the formation of necks within the gage length; two necks are clearly visible in the specimen tested at the lowest strain rate (Specimen J in Fig. 3).

A similar sequence of fracture characteristics was observed at 503 K, but in this case even the fastest strain rate yielded a total strain at failure of ~ 430 pct (Specimen B in Fig. 4). A comparison of Figs. 3 and 4 reveals the similar appearance of Specimen D tested at $1.33 \times 10^{-1} \text{ s}^{-1}$ at 423 K and Specimen B tested at 1.33 s^{-1} at 503 K: as indicated in the plot of σ versus $\dot{\epsilon}$ in Fig. 2, both of these specimens gave similar values for the maximum flow stress. The fracture behavior at the lower strain rates was also similar for these two temperatures (compare Specimens I and J in Figs. 3 and 4), although, as already noted, the lowest testing temperature led to a small but significant increase in the total ductility at failure.

To check the magnitude of grain growth during the long-term tests at low rates of strain, the specimens tested at the highest temperature (503 K) were sectioned near to the point of fracture and measurements were taken to determine the final grain size, d' . In practice, grain growth at an elevated temperature may occur by natural coarsening, which is time dependent, and by deformation-induced coarsening which is dependent on plastic flow, and the rate of flow, in the material. In order to differentiate between these two possibilities, an additional specimen having an initial grain size of $2.5 \mu\text{m}$ was held at a temperature of 503 K without stress for a period of 85 h, corresponding to the time to fracture for the specimen tested at

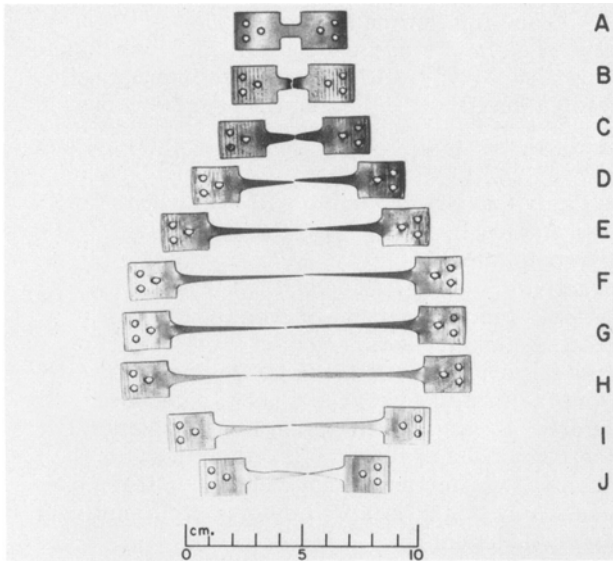


Fig. 3—Tensile specimens having an initial grain size of $2.5 \mu\text{m}$. Specimen A is untested. The other specimens were tested to failure at 423 K at initial strain rates of 1.33 s^{-1} (B), $3.33 \times 10^{-1} \text{ s}^{-1}$ (C), $1.33 \times 10^{-1} \text{ s}^{-1}$ (D), $6.67 \times 10^{-2} \text{ s}^{-1}$ (E), $1.33 \times 10^{-2} \text{ s}^{-1}$ (F), $3.33 \times 10^{-3} \text{ s}^{-1}$ (G), $1.33 \times 10^{-3} \text{ s}^{-1}$ (H), $1.33 \times 10^{-4} \text{ s}^{-1}$ (I), and $1.33 \times 10^{-5} \text{ s}^{-1}$ (J).

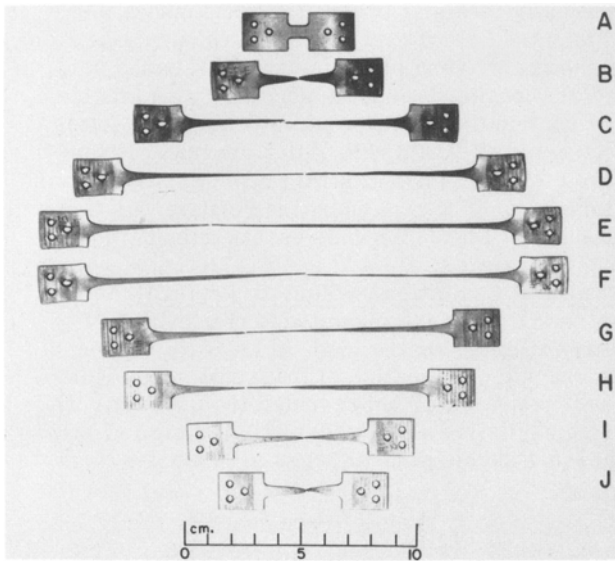


Fig. 4—Tensile specimens having an initial grain size of $2.5 \mu\text{m}$. Specimen A is untested. The other specimens were tested to failure at 503 K at initial strain rates of 1.33 s^{-1} (B), $3.33 \times 10^{-1} \text{ s}^{-1}$ (C), $1.33 \times 10^{-1} \text{ s}^{-1}$ (D), $6.67 \times 10^{-2} \text{ s}^{-1}$ (E), $1.33 \times 10^{-2} \text{ s}^{-1}$ (F), $3.33 \times 10^{-3} \text{ s}^{-1}$ (G), $1.33 \times 10^{-3} \text{ s}^{-1}$ (H), $1.33 \times 10^{-4} \text{ s}^{-1}$ (I), and $1.33 \times 10^{-5} \text{ s}^{-1}$ (J).

the lowest strain rate at this temperature ($1.33 \times 10^{-5} \text{ s}^{-1}$, Specimen J in Fig. 4), and the final grain size was measured as $3.2 \mu\text{m}$.

The results of the grain growth measurements are plotted in Fig. 5 as the normalized change in grain size, $\Delta d/d$, vs $\dot{\epsilon}$, where $\Delta d = d' - d$. The lower point at $\dot{\epsilon} = 1.33 \times 10^{-5} \text{ s}^{-1}$ shows the rather negligible change in grain size due only to natural coarsening in the absence of a stress: the broken curve shows the total change in grain size, due both to natural coarsening and to deformation-induced coarsening.

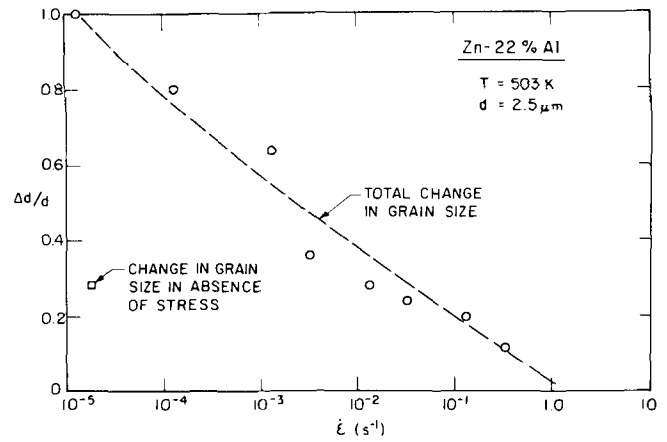


Fig. 5—Normalized change in grain size vs initial strain rate for specimens having an initial grain size of $2.5 \mu\text{m}$ tested at 503 K. The effect of natural coarsening in the absence of a stress is indicated by the lower point at $1.33 \times 10^{-5} \text{ s}^{-1}$.

These results confirm that grain growth is of minor importance in this material in Regions II and III (corresponding to $\dot{\epsilon} \gtrsim 2 \times 10^{-3} \text{ s}^{-1}$), since the maximum increase in grain size in these regions was by a factor of ~ 1.4 for the specimen tested at an initial strain rate of $3.33 \times 10^{-3} \text{ s}^{-1}$ near the lower end of Region II. Grain growth is more important in Region I, but the total increase in grain size was never larger than a factor of two, even for the smallest grain size tested at the highest temperature for the longest period of time ($d = 2.5 \mu\text{m}$, $d' = 5.0 \mu\text{m}$ after 85 h, for $\dot{\epsilon} = 1.33 \times 10^{-5} \text{ s}^{-1}$ at $T = 503 \text{ K}$). By contrast, some other materials used in investigations of superplasticity have exhibited very extensive grain growth during the testing procedure. For example, in experiments on the Al-33 pct Cu eutectic alloy, Rai and Grant⁵ observed increases in grain size of up to, and in excess of, one order of magnitude. The significance of concurrent grain growth is discussed in more detail later.

Effect of Initial Grain Size

The influence of initial grain size on the ductility curves is shown in the upper portion of Fig. 6 for specimens having grain sizes of 2.5 and $4.2 \mu\text{m}$ tested at a temperature of 473 K: the corresponding plots of maximum flow stress vs initial strain rate are shown in the lower portion of Fig. 6.

Although there is again some scatter in the ductility results, three trends are visible:

- i) As the initial grain size is increased, the peak in the curve of $\Delta L/L_0$ vs $\dot{\epsilon}$ occurs at lower strain rates.
- ii) The maximum attainable ductility in the superplastic region increases as the grain size is decreased.
- iii) Maximum ductility occurs with the smallest initial grain size at high strain rates, but at low strain rates this trend is reversed.

To check the magnitude of grain growth when the initial grain size is $4.2 \mu\text{m}$, a specimen was sectioned after fracture at the lowest strain rate and the final grain size was measured as $5.8 \mu\text{m}$. A similar specimen held at 473 K for 85 h in the absence of a stress yielded a final grain size of $4.6 \mu\text{m}$. The maximum grain growth in these specimens was therefore less than a factor of 1.4 at this testing temperature.

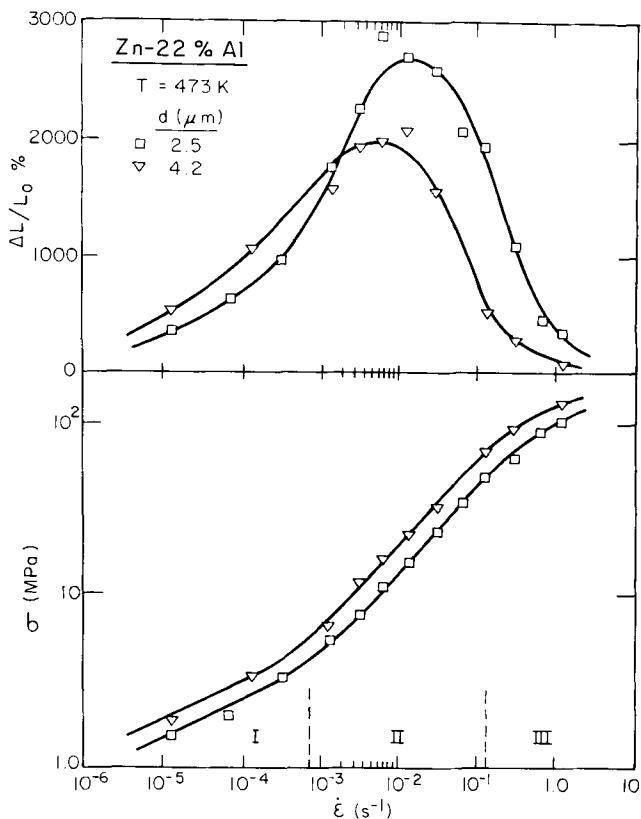


Fig. 6—Tensile fracture strain as a percentage vs initial strain rate for a testing temperature of 473 K and initial grain sizes of 2.5 and 4.2 μm (upper); the corresponding plots of maximum flow stress vs initial strain rate (lower).

DISCUSSION

Effect of Temperature and Grain Size

The ductility curves shown in the upper portions of Figs. 2 and 6 reveal several features which were summarized earlier. In order to interpret these experimental results, it is necessary to consider two factors which affect specimen ductility.

Influence of Strain Rate Sensitivity on Necking. The total ductility observed in a tensile test is greatly influenced by the strain rate sensitivity, since a high value of m leads to a situation in which the necks are diffuse and do not propagate. Under these conditions, the areas of reduced cross-section deform at similar rates to the remainder of the specimen, and the behavior is superplastic. The requirement of a high value of m may be demonstrated by combining Eq. [1] with the definitions of stress

$$\sigma = P/A \quad [2]$$

where P is the tensile force and A is the cross-sectional area, and the strain rate at constant volume

$$\dot{\epsilon} = -(1/A)dA/dt \quad [3]$$

where t is the time, to give

$$-\frac{dA}{dt} = \left(\frac{P}{B}\right)^{1/m} \left(\frac{1}{A(1-m)/m}\right) \quad [4]$$

Eq. [4] shows that dA/dt approaches a common level

as $m \rightarrow 1$, and for Newtonian viscous flow when $m = 1$ the value of dA/dt is independent of A . It is anticipated therefore that $\Delta L/L_0$ will increase with increasing m , and reach a maximum in Region II.* Furthermore, it

*The same general trend also follows from a detailed numerical analysis of plastic instabilities due to the growth of necks.⁶

seems likely that the maximum will occur near the center of Region II, where the influence of Regions I and III is a minimum.

In practice, an examination of Figs. 2 and 6 shows that the peaks in the ductility curves tend to coincide with points which are within Region II but slightly closer to the points of transition to Region I. This effect probably arises because a neck, once developed, will deform at a strain rate which is effectively higher than the remainder of the gage length. Thus, for the specimens exhibiting maximum ductility in these experiments, any slight neck will deform at a point near the center of Region II.*

*As demonstrated in Fig. 6, the peak in the curve of $\Delta L/L_0$ vs $\dot{\epsilon}$ is transposed to lower strain rates for larger initial grain sizes. This suggests the alternative possibility that the occurrence of grain growth tends to shift the peak to lower strain rates. In practice, the data in Fig. 5 indicate that grain growth was minimal (a factor of ~ 1.3) in these experiments in the vicinity of the peak ductility, so that this effect is necessarily of minor importance in the present work.

The effect of relating $\Delta L/L_0$ to m is illustrated schematically in Fig. 7, where the solid curve shows the anticipated behavior at 473 K and the upper broken curve shows the trend predicted at 423 K based solely on the value of the strain rate sensitivity. As indicated, the peak in the ductility curve occurs at a lower value of imposed strain rate with a decrease in temperature. The influence of strain rate sensitivity is therefore capable of explaining the relative positions of the peaks in Fig. 2, but it is unable to explain their relative magnitudes.

Influence of Cavitation on Time to Rupture. To obtain an indication of the magnitudes of ductility, it is necessary to consider the mode of fracture. A recent metallographic examination of fractured specimens of the Zn-22 pct Al eutectoid revealed the presence of extensive cavitation after deformation in the low stress Region I, and significant, although substantially less,

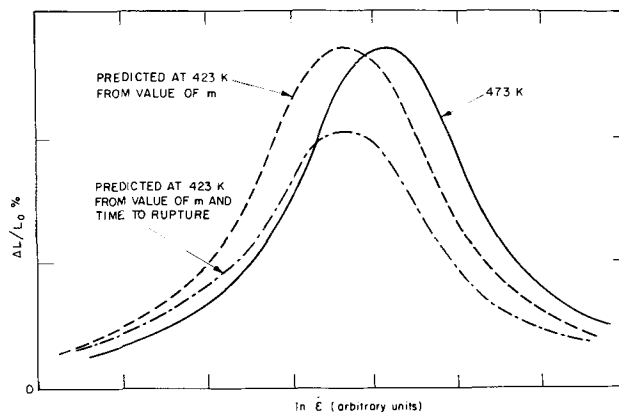


Fig. 7—The solid curve and the upper broken curve show the anticipated behavior at 473 and 423 K, respectively, based solely on the value of the strain rate sensitivity, m . The lower broken curve schematically indicates the anticipated behavior at 423 K when the analysis includes the influence of cavitation on the time to rupture.

cavitation after deformation to ~ 2600 pct in the superplastic Region II.⁷

Unfortunately, the precise role of these cavities is not known at the present time, and it is therefore not possible to quantitatively determine their influence on the total ductility. However, in a qualitative sense the experimental results are consistent with the observed cavitation, since more time is available at the lower strain rates for the cavities to grow and link, thereby decreasing the anticipated time to rupture.

Two additional factors are also consistent with the experimental trends. First, cavities are less likely to form as the temperature is increased, because stress concentrations may be relieved more easily through localized diffusion. This is consistent with the data shown in Fig. 2. Second, it has been demonstrated that fracture occurs by a combination of external necking and an intergranular void sheet process at low strain rates in Region I.⁷ For the latter process, ductility is controlled by the total volume fraction of voids,⁸ and this gives rise to a decrease in ductility with decreasing grain size because of the larger total grain boundary area. This is consistent with the data shown in Fig. 6.

Although it is therefore not possible to calculate precise values for $\Delta L/L_0$ as a function of temperature, the foregoing argument suggests that, when the time to rupture is also considered, there will be a decrease in the anticipated ductility at the lower temperature. This effect is indicated schematically by the lower broken curve for 423 K in Fig. 7.

COMPARISON WITH OTHER INVESTIGATIONS

Despite the considerable current interest in superplasticity, and the large number of experiments conducted on superplastic materials, very few tests have been performed to specifically investigate the factors influencing the total ductility. Furthermore, the results at present available tend to be conflicting.

Taplin and co-workers⁹⁻¹² used various Cu alloys to show that maximum ductility occurred at an intermediate strain rate, of the order of 10^{-3} s^{-1} , and there was a drop in ductility at both higher and lower values of $\dot{\epsilon}$. This trend is therefore similar to the present results, although the Cu alloys were not highly superplastic and the total fracture strains observed in these materials under optimum conditions were < 800 pct. It is interesting to note that one of the sets of data showing this trend was obtained under conditions of constant true strain rate rather than constant cross-head displacement.¹²

Sagat and Taplin¹³ performed experiments on the Pb-Cd eutectic having two different grain sizes. They reported a larger rupture strain in specimens of the smaller grain size, which is again consistent with the present results in Regions II and III (see Fig. 6).

By contrast, Rai and Grant⁵ investigated the fracture characteristics of the Al-33 pct Cu eutectic alloy, and reported that the total strain at fracture continued to increase with decreasing strain rate, down to strain rates of at least 10^{-7} s^{-1} . At first sight, these results appear incompatible with the present data, but closer inspection reveals significant similarities:

i) Rai and Grant⁵ obtained a constant value of m , equal to ~ 0.5 , over the lowest two orders of magnitude

of strain rate used in their work, and, with the exception of data described in the next section, there was no evidence for the existence of Region I. The occurrence of the highest ductility at the lowest strain rate is therefore additional confirmation that $\Delta L/L_0$ reaches a maximum in the region of highest m .

ii) Rai and Grant⁵ observed massive grain growth in their experiments, with increases in grain size up to and exceeding an order of magnitude. For example, the specimen showing maximum elongation (~ 1150 pct) at the highest temperature and lowest strain rate exhibited an increase in grain size from 1.5 to 20 μm . As demonstrated in Fig. 6, even a small increase in the initial grain size leads to a shift in the peak in the ductility curve to a lower strain rate. It is therefore possible that the very large changes in grain size reported for the Al-33 pct Cu eutectic, both at intermediate and very low strain rates, were sufficient to move the peak to the lowest available strain rate. By contrast, only moderate grain growth was observed in the present experiments (≤ 2 times), even at the slowest rates of strain.

iii) Rai and Grant⁵ reported that, for a constant strain rate, the observed ductility increased with increasing temperature. Although this is generally true, and is in agreement with many of the results obtained on Zn-22 pct Al, Fig. 2 shows that a reversal may occur at the low strain rates due to the onset of Region I.

THE EFFECT OF CONCURRENT GRAIN GROWTH

As already noted, the occurrence of grain growth during the tests tends to shift the peak ductility to lower strain rates. In addition, Rai and Grant⁵ reported the appearance of a Region I in some of their experiments, but demonstrated that the trend was false and arose because of substantial grain growth at the very lowest strain rate. Although much less grain growth was observed in the present experiments (see Fig. 5), it is important to check whether the small increase in grain size observed in this work is capable of accounting for the presence of a well-defined Region I.

For the lowest strain rate at 503 K, the maximum flow stress was attained after a testing time of ~ 15 h. Reference to the grain growth data in Fig. 5 suggests that the grain size at this time was probably $\sim 3.0 \mu\text{m}$. Experiments have shown that the strain rate in Region II varies inversely with the grain size raised to a power of ~ 2.3 .¹ Since the stress exponent in this region is ~ 2.2 , the effect of an increase in grain size from 2.5 to 3.0 μm is to introduce an apparent increase in the stress level by the relatively minor factor of ~ 1.2 . By contrast, the experimental stress at this point deviates from a linear extrapolation of Region II by a factor of ~ 4 (see Fig. 2). It is therefore concluded that the occurrence of grain growth is not able to account for the presence of Region I in this material.

Finally, it should be noted that Nicholson¹⁴ has also reported natural and deformation-induced grain coarsening in the Zn-22 pct Al eutectoid, although his tabulated results show the largest grain size occurring in the specimen tested at the *fastest* strain rate for the *shortest* period of time. This contrasts with both the present results on the same material and the observations by Rai and Grant⁵ on the Al-33 pct Cu eutectic

alloy, where maximum grain growth was obtained at the *slowest* testing strain rate after the *longest* period of time. It is suggested that the results of Nicholson¹⁴ are probably not generally representative of superplastic materials, and may arise from using specimens of very small grain size which were not annealed above the testing temperature prior to the experiments. This possibility is partially confirmed by noting that the grain sizes reported by Nicholson¹⁴ were all $< 1 \mu\text{m}$.

SUMMARY AND CONCLUSIONS

1) The maximum attainable ductility in the superplastic Zn-22 pct Al eutectoid depends critically on the imposed strain rate, the testing temperature, and the initial grain size.

2) The ductility reaches a maximum at intermediate strain rates, in the superplastic Region II, but decreases at both higher and lower strain rates. Maximum ductility is observed at higher strain rates as the temperature is increased and/or the grain size is decreased.

3) The maximum attainable ductility increases with increasing temperature and/or decreasing grain size.

4) At high strain rates, maximum ductility occurs at the highest testing temperature and with the smallest initial grain size: at low strain rates, these trends are reversed.

5) For specimens tested at different temperatures, similar macroscopic fracture characteristics are ob-

served in specimens which exhibit a similar maximum flow stress.

6) The experimental trends may be explained, at least qualitatively, by relating maximum ductility to the maximum strain rate sensitivity and examining the influence of cavitation on the time to rupture.

ACKNOWLEDGMENT

This work was supported by the National Science Foundation under Grant No. DMR72-03238 A01.

REFERENCES

1. F. A. Mohamed and T. G. Langdon: *Acta Met.*, 1975, vol. 23, pp. 117-24.
2. F. A. Mohamed, S.-A. Shei, and T. G. Langdon: *Acta Met.*, 1975, vol. 23, pp. 1443-50.
3. H. Ishikawa, F. A. Mohamed, and T. G. Langdon: *Phil. Mag.*, 1975, vol. 32, pp. 1269-71.
4. F. A. Mohamed and T. G. Langdon: *Phil. Mag.*, 1975, vol. 32, pp. 697-709.
5. G. Rai and N. J. Grant: *Met. Trans. A*, 1975, vol. 6A, pp. 385-90.
6. M. A. Burke and W. D. Nix: *Acta Met.*, 1975, vol. 23, pp. 793-98.
7. H. Ishikawa, D. G. Bhat, F. A. Mohamed, and T. G. Langdon: *Met. Trans. A*, 1977, vol. 8A, pp. 523-25.
8. R. G. Fleck, G. J. Cocks, and D. M. R. Taplin: *Met. Trans.*, 1970, vol. 1, pp. 3415-20.
9. G. L. Dunlop and D. M. R. Taplin: *J. Mater. Sci.*, 1972, vol. 7, pp. 84-92.
10. S. Sagat, P. Blenkinsop, and D. M. R. Taplin: *J. Inst. Metals*, 1972, vol. 100, pp. 268-74.
11. D. M. R. Taplin and S. Sagat: *Mater. Sci. Eng.*, 1972, vol. 9, pp. 53-55.
12. S. Sagat and D. M. R. Taplin: *Acta Met.*, 1976, vol. 24, pp. 307-15.
13. S. Sagat and D. M. R. Taplin: *Met. Sci.*, 1976, vol. 10, pp. 94-100.
14. R. B. Nicholson: *Electron Microscopy and Structure of Materials*, G. Thomas, ed., pp. 689-719, University of California Press, Berkeley, 1972.